Supporting Information for a Manuscript Entitled:

Composition-dependent Trap Distributions in CdSe and InP Quantum Dots Probed Using Photoluminescence Blinking Dynamics

Heejae Chung,[†] Kyung-Sang Cho,[‡] Weon-Kyu Koh,[,‡] Dongho Kim,[*,†] and Jiwon Kim [*,§]*

[†] Department of Chemistry and Spectroscopy Laboratory for Functional π-Electronic Systems, Yonsei University, 262 Seongsanno, Seodaemun-gu, Seoul 03722, Republic of Korea.

[‡] Device Laboratory, Device and System Research Center, Samsung Advanced Institute of Technology, Samsung Electronics, 130 Samsung-ro, Yeongtong-gu, Suwon-si, Gyeonggi-do 16678, Republic of Korea.

[§] School of Integrated Technology, Yonsei Institute of Convergence Technology and Underwood International College, Yonsei University, 85 Songdogwahak-ro, Yeonsu-gu, Incheon 21983, Republic of Korea.

Supporting Information

1. Basic Properties of QDs.

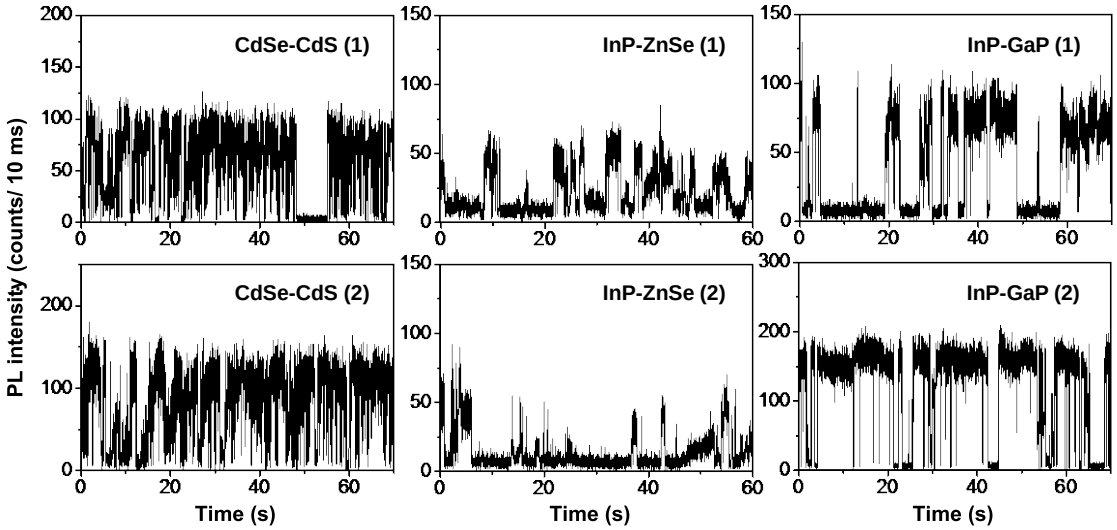

Figure S1. Additional blinking traces for individual QDs: **CdSe-CdS**, **InP-ZnSe**, and **InP-GaP**.

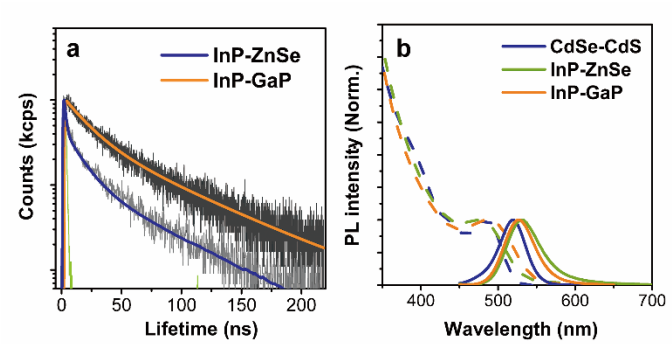

Figure S2. (a) PL decay profiles recorded after excitation at 420 nm for **InP-ZnSe** (blue) and **InP-GaP** (orange) films using a time-correlated single photon counting (TCSPC) technique. GaP shell passivation more efficiently removes the carrier quenching defects (traps) at the interface than ZnSe shell, thereby increasing the amplitude for the slow decay component. (b) Steady-state absorption and photoluminescence spectra for **CdSe-CdS** (blue), **InP-ZnSe** (green), and **InP-GaP** (orange).

2. Fluorescence Lifetime Intensity Distributions.

The blinking behaviors of the QDs were characterized by correlating their PL lifetimes and intensities. Single photon detection events can be monitored in absolute time, thus capturing their relative position to the excitation pulse in the photon stream. This technique allows a sub-histogram to be constructed from the selected portion in the photon stream, making it possible to determine whether the decay dynamics change over time or are correlated with other observables such as integrated intensity. Two-dimensional histograms for the PL lifetimes and intensities referred to as fluorescence lifetime–intensity distributions (FLIDs) were plotted. The FLID plots can be categorized into two types: (a) there is a PL intensity–lifetime correlation, A-type; and (b) changes in the PL lifetime are not accompanied by changes in the PL intensity, B-type.[1] Figure 3a is a representative FLID plot for **InP-GaP**, which shows A-type blinking. The shorter PL lifetimes (a few nanoseconds) of A-type blinking are attributed to Auger recombination, which opens up a fast non-radiative decay channel. The *on*-time probability distribution for A-type blinking shows an exponential truncation (Figure S3). On the contrary, the distribution for B-type blinking follows a power law behavior (Figure S4). Accordingly, it is likely that the exponential truncation, shown as the fall-off time ($\tau_{fall\text{-}off}$), is closely related to the Auger process.

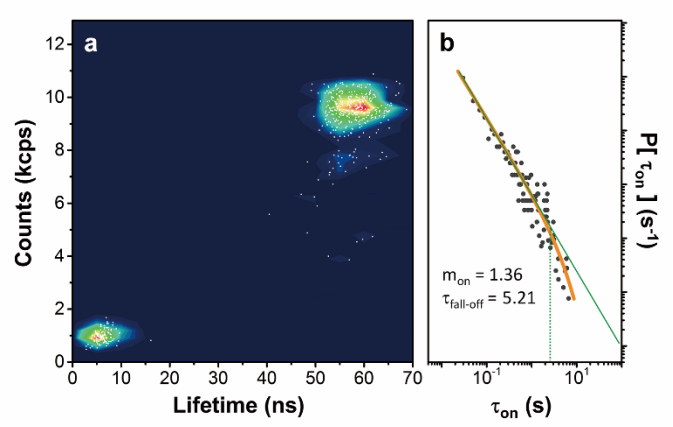

Figure S3. (a) Fluorescence lifetime–intensity distribution (FLID) map for a single **InP-GaP** QD excited at 420 nm, (b) Statistical *on*-time probability distribution for A-type blinking in FLID maps of individual **InP-GaP** QDs. The orange solid line is a fit to the data, as described in the text; the green lines indicate the power law components from the fit of the *on*-time distribution.

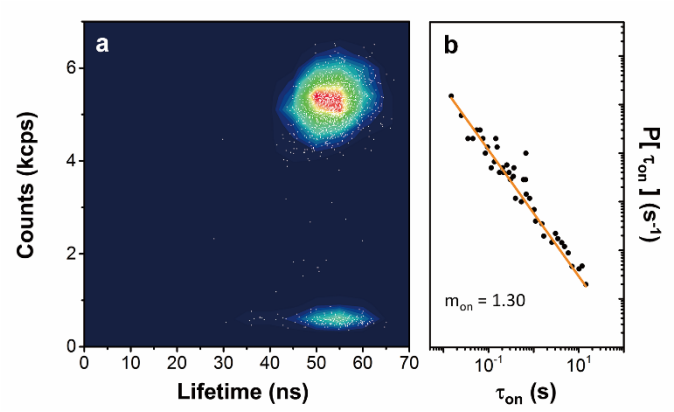

Figure S4. (a) FLID map for a single **InP-GaP** QD excited at 420 nm. (b) Statistical *on*-time probability distribution for B-type blinking in the FLID maps of individual **InP-GaP** QDs.

3. Estimation of Multiexciton (MX) Creation Times $\langle t_{MX} \rangle$.

Schematic description of the single exciton (SX) or multiexciton (MX) creation process upon pulsed photoexcitation:

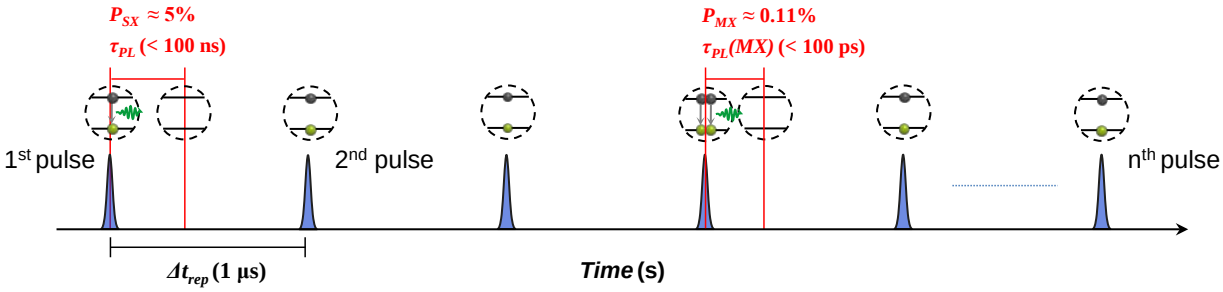

1) The multiexcitonic species are generated much less frequently than the single excitonic species because the probability of creating multiexciton per pulse (P_{MX}) is much lower than the probability for single-exciton (P_{SX}). **2)** However, every single pulse can generate multiexciton with an extremely small probability P_{MX} (≈ 0.11%) regardless of the photoluminescence lifetime of single or multiexcitonic spicies ($\tau_{PL}(SX)$ and $\tau_{PL}(MX)$, respectively) in QDs.

1) Exciton decays before the next pulse comes in: Since the PL lifetime of single exciton is much shorter than the laser repetition time (Δt_{rep}; 1 μs), multiexcitonic species cannot be generated by a re-excitation process.

2_a) Single pulse generates multiexciton[2,3-6]: The average number of created excitons $\langle N_x \rangle$ can be calculated in a straight forward manner using the absorption cross section (σ, cm^{-2}) of the QD at the excitation wavelength and the intensity of laser (j, photons/cm^2·pulse) ($\langle N_x \rangle = j\sigma$. Considering the creation of 'n' excitons as an independent event, the probability of creating 'n' excitons per pulse (P_{NX}) is given by a Poisson distribution (n is an integer greater than or equal to 0).

$$P_{\langle N_x \rangle}(n) = e^{-\langle N_x \rangle} \cdot \langle N_x \rangle^n / n! \qquad (1)$$

Thus, the probability of the multiexciton creation per pulse (P_{MX}) can be expressed as

$$1 - e^{-\langle N_x \rangle} - \langle N_x \rangle \cdot e^{-\langle N_x \rangle} \qquad (2)$$

, where second (P_{ZX}) and third (P_{SX}) terms indicate the probability of creating '*n*' excitons when *n* = 0 and 1, respectively. This expression is addressed in the work of *Nano Lett.*, 2009, 9, 338–345 (ref. 51) and also elsewhere (ref. 55-58 in the Manuscript). According to the equation (1) and (2), the P_{MX} is quite low (0.11%, 1.01% and 0.83% for **CdSe-CdS**, **InP-ZnSe** and **InP-GaP** QDs, respectively) but not zero for all samples under the given excitation conditions (420 nm, 70 W/cm^2). Moreover, zero-time coincidence feature in $g^{(2)}(\tau)$ measurements under weak pulsed excitation conditions (≈ 70 W/cm^2) can solely be understood by multiexciton decay.

2_b) Although P_{MX} (≈ 0.11%) is much lower than P_{SX} (≈ 5%), we cannot neglect an impact of the multiexcitonic species under a large number of trials (*n*; *n* = 10,000): This is most convincingly illustrated in terms of a probability ($P_r(k)$) of forming '*r*' multiexcitonic species in a function of '*k*' number of trials (both *r* and *k* are integers greater than or equal to 1).

As shown in Figure S5, $P_r(k)$ increases and finally converges to 1 as the number of trials *k* increases. For the average excitation rate of 1 MHz, multiexciton is generated with unity probability over a time period of 1 ms (*n* = 1,000) for all samples. If creation of multiexcitonic species upon excitation is a successful event and the others (getting zero or single exciton) are considered to be failures, we can evaluate the average number of getting multiexcitonic species by multiplying '*k*' and P_{MX}. Thus, when every 10,000 pulses (10 ms) are detected to be a signal, the probability of multiexciton creation (and its impact in the blinking process) is not negligible.

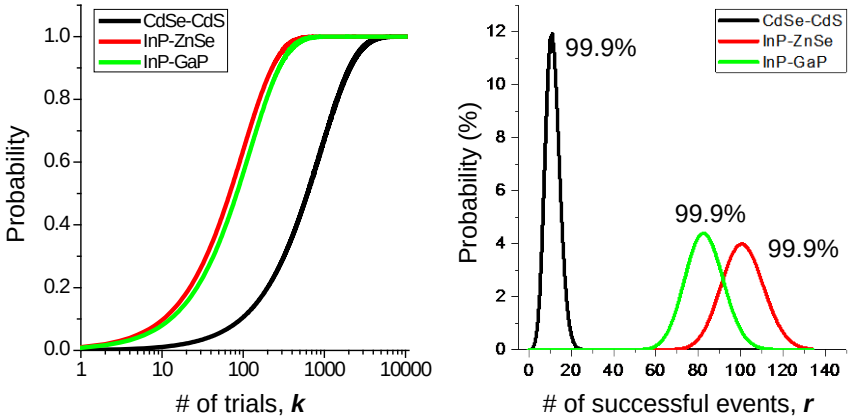

Figure S5. Simple Poisson statistics demonstrates that the formation of multiexcitonic species is a highly probable event on a millisecond time scales ($k \geq 10{,}000$, k is the number of trials). We plotted the probabilities ($P_r(k)$) of creating multiexcitonic species at least once out of k trials as a function of k (*left*): $P_r(k)(r \geq 1)$ can be expressed as $1-(1-P_{MX})^k$. The probability of getting exactly 'r' multiexcitonic species out of 10,000 trials is calculated by using equation 3 (*right*). The probability distribution shows a maximum at the expectation value (kP_{MX}) when there are k trials for each QD. The total probability $P_r(k)(r \geq 1)$ is almost unity ($\approx$ 99.9%).

Poisson distribution is one of the Binomial distribution and thereby the probability of getting exactly 'r' successes in k trials can be given by the probability mass function: if 'r' is the number of successful trials, the probabilities for exactly 'r' successes and 'k-r' failures are $(P_{MX})^r$ and $(1- P_{MX})^{k-r}$, respectively. However, the 'r' successes can occur any time out of k trials. Thus, $P_r(k)$ can be expressed as follows:

$$P_r(k)=\binom{k}{r} P_{MX}{}^r(1-P_{MX})^{k-r} \qquad (3)$$

, where P_{MX} is the success probability in each trial.

We calculated the characteristic 1/e time of forming any multiexcitonic species (tau_MX) in the same manner as the work of *Nano Lett.*, 2009, 9, 338–345. The multiexciton creation time (tau_MX) can be translated into the number of trials k. Under a given trials k (the number of trials k is 892, 99 and 120 for **CdSe-CdS**, **InP-ZnSe** and **InP-GaP** QDs, respectively), the expectation values are 1 for all samples with a probability of 36.9 % (1/e %). Thus, whether

the PL lifetime is shorter or longer than the tau_MX, the multiexciton can easily be generated at least once during a given bin time if the bin time is longer than tau_MX.

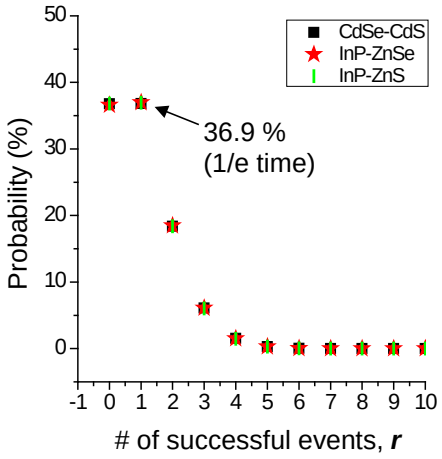

Figure S6. The probability of exactly one multiexcitonic species upon photo-illumination over $\langle t_{MX} \rangle$ is 36.9% (1/*e* %).

4. Estimation of Biexciton (BX) PL Quantum Yields.

To calculate the BX PL quantum yields, second-order intensity correlation ($g^{(2)}(\tau)$) analyses were performed under pulsed excitation. In general, the peak at zero-time gives the number of the coincident photon pairs and all the other peaks give the number of photon pairs when individual photons originate from different excitation pulses. Previous reports have indicated that the normalized area of the zero-time coincidence feature in $g^{(2)}(\tau)$ measurements is approximately the same as the ratio of BX to SX PL quantum yields (η_{BX}/η_{SX}) under weak excitation conditions.[7,8] Therefore, the η_{BX}/η_{SX} values were calculated by dividing the integrated central areas by the average of six integrated peaks (marked 1 to 6 in Figure S5). The time interval between the nearest neighbor peaks is 1 μs, which corresponds to the inverse laser pulse repetition rate.

Assuming the center value of a Gaussian fit ($I_{QD(reference)}$) represents the PL quantum yield ($\eta_{SX,QD(reference)}$) measured using ensemble spectroscopy (Figure S6), the ratio between the PL

intensities of two individual QDs can be used as a correction factor ($\frac{\eta_{SX,QD(reference)} \cdot I_{QD(object)}}{I_{QD(reference)}}$) to calculate the SX PL quantum yield for each QD. The BX PL quantum yield can be obtained using the following equations:

$$\frac{I_{QD(reference)}}{I_{QD(object)}} = \frac{\eta_{SX,QD(reference)}}{\eta_{SX,QD(object)}}, \quad (1)$$

$$\eta_{BX,QD(object)} = \frac{\eta_{BX,QD(object)}}{\eta_{SX,QD(object)}} \times \eta_{SX,QD(reference)} \times \frac{I_{QD(object)}}{I_{QD(reference)}}. \quad (2)$$

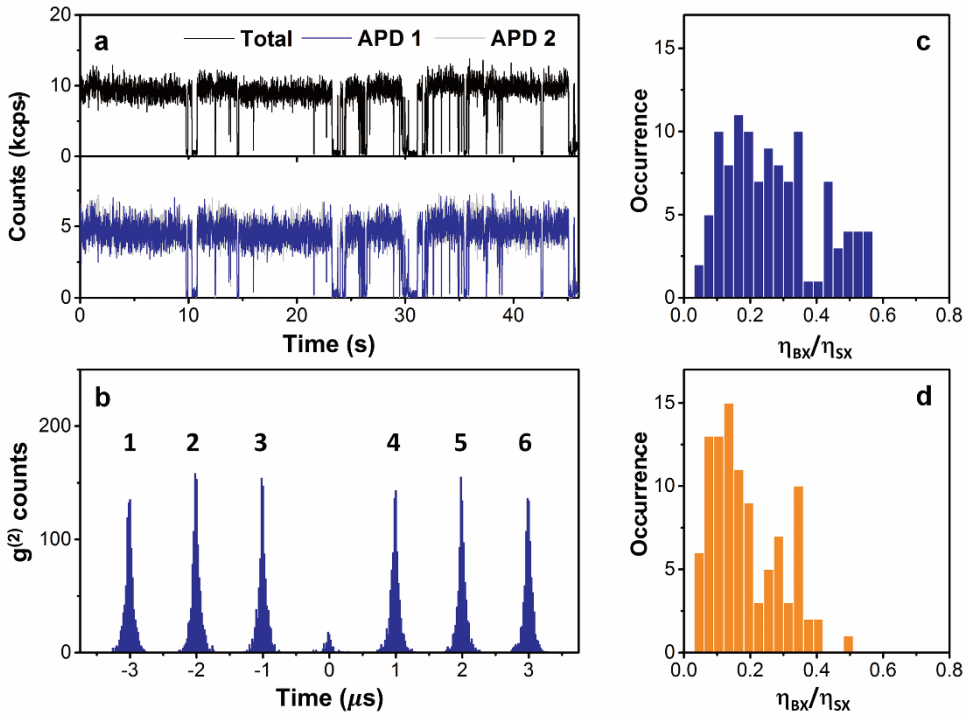

Figure S5. (a) Representative PL blinking traces for **InP-GaP** in the start and stop channels during $g^{(2)}$ acquisition and (b) measured $g^{(2)}(\tau)$ values for a single QD with pulsed excitation. (c, d) Histograms of the biexciton (BX) to single exciton (SX) PL quantum yield ratios for **CdSe-CdS** (blue) and **InP-GaP** (orange).

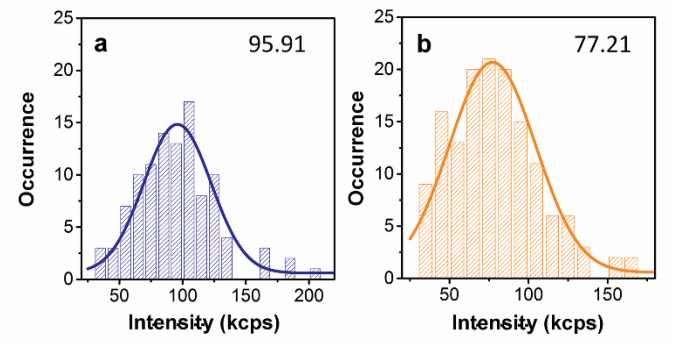

Figure S6. PL intensity histograms for (a) **CdSe-CdS** (blue) and (b) **InP-GaP** (orange) follow Gaussian statistics; the center value of the Gaussian fit represents the PL quantum yield determined using ensemble spectroscopy.

REFERENCES

(1) Galland, C.; Ghosh, Y.; Steinbrück, A.; Sykora, M.; Hollingsworth, J. a.; Klimov, V. I.; Htoon, H. Two Types of Luminescence Blinking Revealed by Spectroelectrochemistry of Single Quantum Dots. *Nature* **2011**, *479*, 203–207.

(2) J. J. Peterson and D. J. Nesbitt, Nano Lett., 2009, 9, 338–345.

(3) C. Galland, Y. Ghosh, A. Steinbrück, M. Sykora, J. A. Hollingsworth, V. I. Klimov and H. Htoon, Nature, 2011, 479, 203–207.

(4) Y. S. Park, W. K. Bae, J. M. Pietryga and V. I. Klimov, ACS Nano, 2014, 8, 7288–7296.

(5) G. Nair, J. Zhao and M. Bawendi, Nano Lett., 2011, 11, 1136–1140.

(6) J. Zhao, O. Chen, D. B. Strasfeld and M. G. Bawendi, Nano Lett., 2012, 12, 4477–4483.

(7) Nair, G.; Zhao, J.; Bawendi, M., *Nano Lett.* **2011**, 1136–1140.

(8) Zhao, J.; Chen, O.; Strasfeld, D. B.; Bawendi, M. G., *Nano Lett.* **2012**, *12*, 4477–4483.